JOURNAL OF ENGINEERING annals OF FACULTY OF ENGINEERING HUNEDOARA

A STUDY OF THE BOCKER'S OBSERVER IMPLEMENTATION TO ESTIMATE THE INDUCED POWER WITHIN A CAST-IRON CONVEYANCE AND DOSAGE ELECTROMAGNETIC PUMP

Adrian DĂNILĂ

Transylvania University of Braşov, ROMANIA

Abstract:
In this paper the structural elements and applications of the electromagnetic pumps for melted cast iron conveyance and dosage within the metallurgical engineering are presented. The mathematical model in steady-state operation of the electromagnetic pump is deduced within Chapter 2. Based on this model, the physical parameters of the melted metal may be estimated. The vector-matrix representation of the dynamic set of equations of the pump is then used, in Chapter 3 to obtain the Bocker's observer. This observer allows to reconstruct the flux-linkages of the magnetic field. Based on these results an estimate of the induced power is sibsequently obtained. At the end of the paper, an implementation of this approach on a given electromagnetic pump is presented
Keywords:
electrothermy, electromagnetic pump, state observers

1. INTRODUCTION

The implementation of the Electro-thermal processes within foundries and forge departments is an important element to improve the products quality and to optimize the energy costs. A modern approach for the conveyance and dosage of melted metals, cast-iron, aluminum, copper and so is the useage of the electromagnetic pumps, Figure 1. The electromagnetic pumps may be used [1] to extract the melted metal directly from the basis of the induction furnace with a not mobile structure and to cast and dose the melted metals from the mobile melting pot. The electromagnetic pumps may be easily inserted into complex plants for continuous casting.

The advantages of the electromagnetic conveyance of melted metals are: (1) the control by electrical means of the liquid's flow-rate if the pump is supplied from controlled three-phased frequency converters, (2) costs reduction due to the elimination of purging the channel with tempered metal scraps, (3) the increase of the metal's pureness because the non-metallic elements aren't drawn by the electromagnetic forces, (4) the melting furnace and the melting pot may be at the same level thus their structure is much simpler, and (5) an improve of the working conditions within the casting departments.

The main disadvantage of the electromagnetic pump is the channel maintenance especially to the channel's basis where the material is highly solicited.

The induction electromagnetic pump is an induction motor with a two-sided or single-sided stator. The main parts of an induction electromagnetic pump with single-sided stator are, Figure 2. The magnetic circuitry 4 with the three-phased winding 3 are placed below the ascending channel 1, build with refractory cement concrete. The melted metal 2 flows through the channel due to the electromagnetic forces. The main technical characteristics of some widely used electromagnetic pumps are presented in Table 1.

Figure 1. An electromagnetic pump for casting melted cast-iron.

2. THE MATHEMATICAL MODEL OF THE SINGLE-SIDED-STATOR ELECTROMAGNETIC PUMP

The stator winding of the induction electromagnetic pump supplied from a three-phased electric network produces a progressive electromagnetic field, Figure 3. The first harmonic of the resulting electromagnetic field above the single-sided stator is given by the following expression:

$$B_{\delta}(x,t) = B_{\delta m} \cdot sin\left(\omega_1 \cdot t - \frac{\pi}{\tau} \cdot x\right) \quad (1)$$

where: $B_{\delta m}$ - the magnitude of the magnetic induction, $\omega_1 = 2 \cdot \pi \cdot f_1$ - the angular frequency and the frequency of the voltages at the stator windings, τ - the stator's winding polar step.

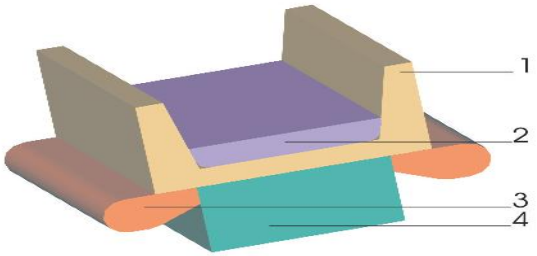

Figure 2. A Simplified cross-section through an electromagnetic pump, single-sided stator.

Table 1
The main features of the electromagnetic pumps

Denomi-nation	Units	Lighte metals	Heavy metals	Cast-iron
Tempe-rature	°C	650 – 750	900 – 1200	1450
Flow rate	kg/s	0,1 – 10	0,3 – 30	1,3 – 100
Level	mm	50 – 540	80 – 540	80 – 930
Length	mm	1080 - 2600	1800 - 2600	1800 - 4200

The motion speed of the first harmonic of the progressive wave, v_1 is:

$$v_1 = \frac{\Delta x}{\Delta t} = 2 \cdot \tau \cdot f_1 \quad (2)$$

The progressive magnetic field induces into the melted metal electric electrical currents due to the electromagnetic induction phenomenon. From the interaction between the resulting magnetic field and the induced currents, electromagnetic force results. This force acts on the melted metal. The electromagnetic force over a unit volume of melted metal may be computed with the relation:

$$\overline{f} = \overline{J} \times \overline{B} \quad (3)$$

where: $\overline{J}$ - the per-unit induced currents and $\overline{B}$ – the induction of the resulting magnetic field into the melted metal.

The expressions of the physical variables of the progressive field and the electromagnetic force, respectively may be deduced through the Maxwell's equations into the space above the inductor –l the air gap of the electromagnetic pump such as for the classical electric machines. In addition, for the induction electro-magnetic pumps the following phenomena have to be taken into account: the transversal edge effect, and the longitudinal edge effect (static and dynamic).

The transversal edge effect consists in the modification of currents distribution through the transversal cross-section of the massive induced because the currents paths freely encircle the magnetic field.

The electro-magnetic force results less than the classical machines provided with windings on both armatures. The decrease of the electromagnetic force depends on the ratio between the polar step and the geometrical dimensions of the induced cross-section within the field, Figure 4.

The transversal edge is taken into account in the electrical equivalent diagram through an additional coefficient that increases the value of the equivalent induced resistance.

The static longitudinal edge effect is because the stator windings aren't balanced – linear stator. The phenomenon consists in a non-symmetrical currents sequence in the stator's windings.

If the magnitudes of the phase voltages are known through measurements and the electric and magnetic parameters are estimated through computations, than the direct- and inverse phase sequence of the stator currents may be determined with the following set of equations:

$$\begin{cases} (3 \cdot \underline{Z}_d + j \cdot 4 \cdot X_0) \cdot \underline{I}_d + (3 \cdot \underline{Z}_i + j \cdot 4 \cdot X_0) \cdot \underline{I}_i = \underline{U}_{AB} - \underline{U}_{CA} \\ \underline{Z}_d \cdot \underline{I}_d - \underline{Z}_i \cdot \underline{I}_i = \frac{j}{\sqrt{3}} \cdot \underline{U}_{BC} \end{cases} \quad (4)$$

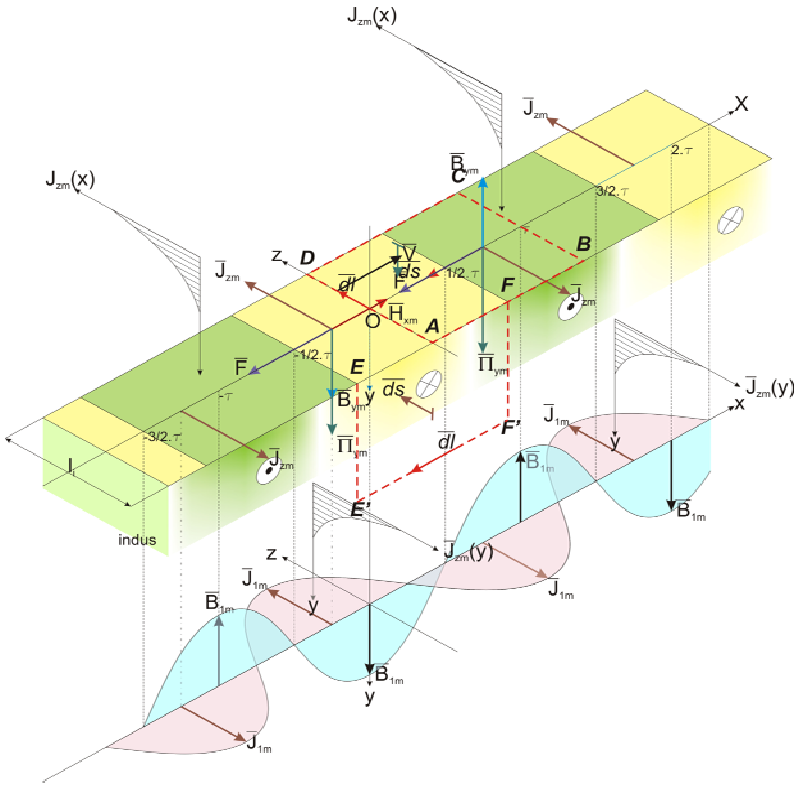

Figure 3. The distribution of the progressive field's first harmonic within the air gap of the electromagentic pump.

A practical approximation is: $\underline{Z}_d = \underline{Z}_i = \underline{Z}_1$. In the relations (4) the significance of the terms is: $\underline{Z}_d, \underline{Z}_i, \underline{Z}_1$ - - the stator direct- and inverse-phase sequence impedances respectively, $\underline{I}_d, \underline{I}_i$ - the symmetrical components of the stator phase currents, X_0 - reactanța totală de dezechilibru şi $\underline{U}_{AB}, \underline{U}_{BC}, \underline{U}_{CA}$ the unbalanced total reactance and - the stator phase voltages.

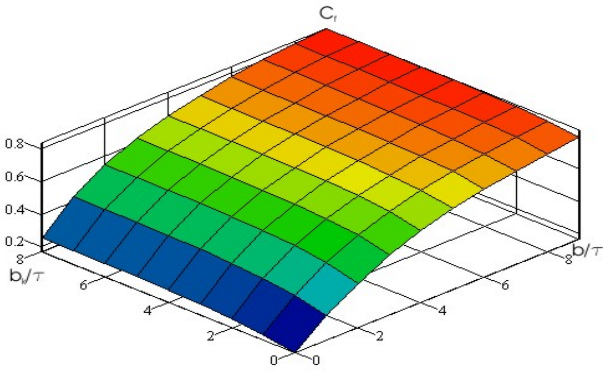

Figure 4. The dependencies of the induced resistance's coefficient

The dynamic longitudinal edge effect consists in the modification of currents distribution along the longitudinal direction.

This is due to the induced motion with respect to the progressive magnetic field.

If the induced reaction is weak then the static longitudinal edge effect on the non-symmetrical system of currents will be preponderant.

The electrical equivalent diagram on a phase of the induction electromagnetic pump may be deduced by integrate the Maxwell's equations into the space above the single-sided stator.

To perform this operation, the vector magnetic potential, $\underline{\Psi}$ has to be used with the boundary conditions on the surfaces between the layers within the pump's air gap:

$$\frac{d^2\underline{\Psi}}{dz^2} - \underline{\beta}^2 \cdot \underline{\Psi} = 0, \quad \underline{\beta} = \sqrt{\left(\frac{\pi}{\tau}\right)^2 + j \cdot \frac{s \cdot \omega_1 \cdot \mu_0}{k_r \cdot \rho}} \tag{5}$$

where: s – the slip, μ_0 - the vacuum magnetic permeability, ρ - the melted metal resistivity, k_r - the resistance's coefficient due to the transversal edge effect.

An equivalent electric diagram is obtained through cascade connection of equivalent elements corresponding to the air gap layers, Figure 5.

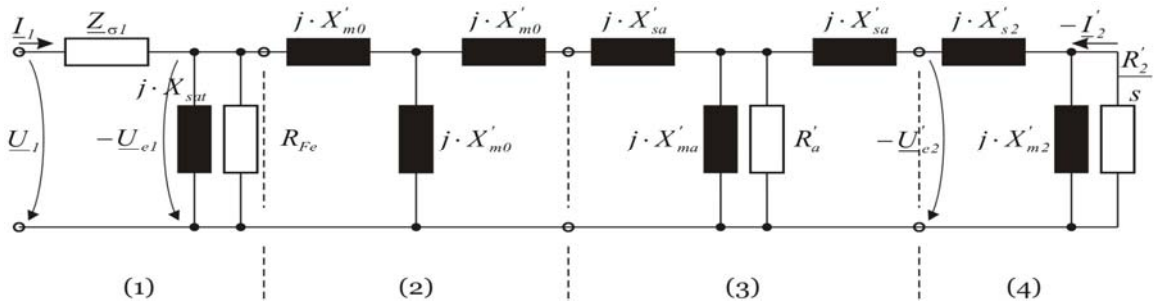

Figure 5. The equivalent electrical diagram of the electromagnetic pump, single-sided stator: (1) – stator, (2) – air, (3) – channel, (4) – melted liquid (induced).

For the on-line computations i.e. adaptive control, the simplified electrical equivalent diagram, Figure 6, is to be used; the significance of the components in Figure 6 is as follows: $\underline{Z}_{\sigma 1}$ - the leakage inductance with respect to the induced, X_m - the linkage inductance, R_{Fe}, R'_a - the equivalent resistances corresponding to the cast-iron and channel losses respectively R'_2 - the equivalent resistance of the induced and s - the slip. The simplified diagram is only valid for larger polar step inductors at low frequencies.

If the pump is supplied from frequency converters, the constant stator flux operation is to be used. In this operation the converter provides a voltage direct phase-sequence with variable magnitude and variable frequency such as $U_1 / f_1 = const.$

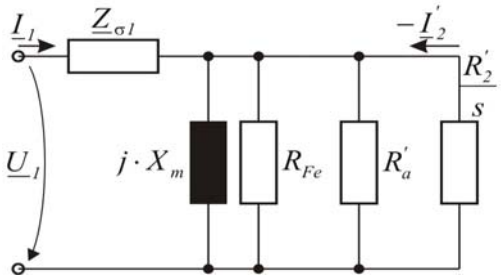

Figure 6. The simplified equivalent electrical diagram of the electromagnetic pump.

In this case the reference coordinate system is referred to the stator.

To obtain an estimate of the induced power into the melted metal the induced currents components and the magnetic flux-linkages components into the induced are to be computed.

The reference coordinate system is the stator and the inputs are the voltages and the currents through the stator winding.

3. IMPLEMENTATION OF BOCKER OBSERVER FOR DETERMINATION OF THE TRANSFERRED POWER TO THE MELTED METAL

The Bocker's observer provides an estimate of the magnetic flux linkages components, [3]. The voltages equations and the flux-linkages equations of the two-phased equivalent system represented in a coordinate system related to the stator are given by the following expressions, [4]:

$$\begin{aligned} u_{d1} &= R_1 \cdot i_{d1} + \frac{d\Psi_{d1}}{dt} \\ u_{q1} &= R_1 \cdot i_{q1} + \frac{d\Psi_{q1}}{dt} \\ 0 &= R'_2 \cdot i'_{d2} + \frac{d\Psi'_{d2}}{dt} + \frac{\pi}{\tau} \cdot v \cdot \Psi'_{q2} \\ 0 &= R'_2 \cdot i'_{q2} + \frac{d\Psi'_{q2}}{dt} - \frac{\pi}{\tau} \cdot v \cdot \Psi'_{d2} \end{aligned} \qquad (6 - 9)$$

$$\begin{aligned} \Psi_{d1} &= L_1 \cdot i_{d1} + L_h \cdot i'_{d2} \\ \Psi_{q1} &= L_1 \cdot i_{q1} + L_h \cdot i'_{q2} \\ \Psi'_{d2} &= L'_2 \cdot i'_{d2} + L_h \cdot i_{d1} \\ \Psi'_{q2} &= L'_2 \cdot i'_{q2} + L_h \cdot i_{q1} \end{aligned} \qquad (10 - 13)$$

From the (10 - 13) set of equations the currents are expressed. Afterwards the results are introduced into the relations (6 - 9). The following set of equations is then obtained:

$$\frac{d\Psi_{d1}}{dt} = -R_1 \cdot \frac{1}{\sigma \cdot L_1} \cdot \Psi_{d1} + R_1 \cdot \frac{1-\sigma}{\sigma \cdot L_h} \cdot \Psi'_{d2} + u_{d1}$$
$$\frac{d\Psi_{q1}}{dt} = -R_1 \cdot \frac{1}{\sigma \cdot L_1} \cdot \Psi_{q1} + R_1 \cdot \frac{1-\sigma}{\sigma \cdot L_h} \cdot \Psi'_{q2} + u_{q1} \qquad (14 - 17)$$
$$\frac{d\Psi'_{d2}}{dt} = R'_2 \cdot \frac{1-\sigma}{\sigma \cdot L_h} \cdot \Psi_{d1} - R'_2 \cdot \frac{1}{\sigma \cdot L'_2} \cdot \Psi'_{d2} - \frac{\pi}{\tau} \cdot v \cdot \Psi'_{q2}$$
$$\frac{d\Psi'_{q2}}{dt} = R'_2 \cdot \frac{1-\sigma}{\sigma \cdot L_h} \cdot \Psi_{q1} - R'_2 \cdot \frac{1}{\sigma \cdot L'_2} \cdot \Psi'_{q2} + \frac{\pi}{\tau} \cdot v \cdot \Psi'_{d2}$$

Subsequently the given set of equations is rewritten in the matrix form as follows:

$$\begin{cases} \frac{d\hat{X}}{dt} = A \cdot \hat{X} + B \cdot U \\ \hat{Y} = C \cdot \hat{X} \end{cases} \qquad (18 - 19)$$

where:

$$A = \begin{bmatrix} -\frac{R_1}{\sigma \cdot L_1} & 0 & \frac{R_1 \cdot L_h}{\sigma \cdot L_1 \cdot L'_2} & 0 \\ 0 & -\frac{R_1}{\sigma \cdot L_1} & 0 & \frac{R_1 \cdot M}{\sigma \cdot L_1 \cdot L'_2} \\ \frac{R_1 \cdot L_h}{\sigma \cdot L_1 \cdot L'_2} & 0 & -\frac{R'_2}{\sigma \cdot L'_2} & -\frac{\pi}{\tau} \cdot v \\ 0 & \frac{R_1 \cdot L_h}{\sigma \cdot L_1 \cdot L'_2} & +\frac{\pi}{\tau} \cdot v & -\frac{R'_2}{\sigma \cdot L'_2} \end{bmatrix}, \quad B = \begin{bmatrix} 1 & 0 \\ 0 & 1 \\ 0 & 0 \\ 0 & 0 \end{bmatrix},$$

$$C = \begin{bmatrix} \frac{1}{\sigma \cdot L_1} & 0 & -\frac{1-\sigma}{\sigma \cdot L_h} & 0 \\ 0 & \frac{1}{\sigma \cdot L_1} & 0 & -\frac{1-\sigma}{\sigma \cdot L_h} \end{bmatrix} \text{ and the vectors: } \hat{X} = \begin{bmatrix} \Psi_{d1} \\ \Psi_{q1} \\ \Psi'_{d2} \\ \Psi'_{q2} \end{bmatrix}, U = \begin{bmatrix} u_{d1} \\ u_{q1} \end{bmatrix}, Y = \begin{bmatrix} i_{d1} \\ i_{q1} \end{bmatrix}.$$

This set of equations is also called the Bocker's observer.

The maximum of the induced reaction is achieved when the melted metal doesn't move, i.e. the induced speed is at zero with respect to the stator, $v = 0$. This approximation may also be used in normal operation of the pump because the speed of the melted metal is usually much smaller than the synchronous speed of the pump. For example, for a given unit the synchronous speed is $v_1 = 19{,}8\ m/s$, while at rated (or nominal) operation the speed of the melted metal results $v_N = 0{,}8\ m/s$.

The system of differential equations (18 - 19) is to be transformed into a system of difference equations with the sampling period T_e and follows the following recursive equations:

$$\begin{bmatrix} \Psi_{d1}(k+1) \\ \Psi_{q1}(k+1) \\ \Psi'_{d2}(k+1) \\ \Psi'_{q2}(k+1) \end{bmatrix} = \begin{bmatrix} 1 - T_e \cdot \frac{R_1}{\sigma \cdot L_1} & 0 & T_e \cdot \frac{R_1 \cdot L_h}{\sigma \cdot L_1 \cdot L'_2} & 0 \\ 0 & 1 - T_e \cdot \frac{R_1}{\sigma \cdot L_1} & 0 & T_e \cdot \frac{R_1 \cdot M}{\sigma \cdot L_1 \cdot L'_2} \\ T_e \cdot \frac{R'_2 \cdot L_h}{\sigma \cdot L_1 \cdot L'_2} & 0 & 1 - T_e \cdot \frac{R'_2}{\sigma \cdot L'_2} & 0 \\ 0 & T_e \cdot \frac{R'_2 \cdot L_h}{\sigma \cdot L_1 \cdot L'_2} & 0 & 1 - T_e \cdot \frac{R'_2}{\sigma \cdot L'_2} \end{bmatrix} \cdot \begin{bmatrix} \Psi_{d1}(k) \\ \Psi_{q1}(k) \\ \Psi'_{d2}(k) \\ \Psi'_{q2}(k) \end{bmatrix} + \qquad (20)$$

$$+ T_e \cdot \begin{bmatrix} 1 & 0 \\ 0 & 1 \\ 0 & 0 \\ 0 & 0 \end{bmatrix} \cdot \begin{bmatrix} u_{d1}(k) \\ u_{q1}(k) \end{bmatrix}$$

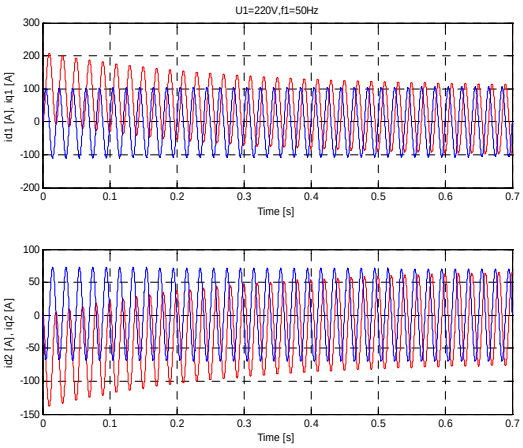

Figure 8. The currents components at start-up and in steady-state operation. Above: stator, below induced.

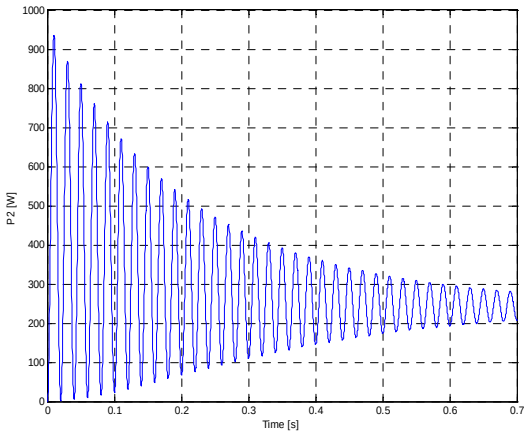

Figure 9. The transferred power to the induced at start-up and in steady-state operation- rated frequency.

$$\begin{bmatrix} i_{d1}(k) \\ i_{q1}(k) \end{bmatrix} = \begin{bmatrix} \frac{1}{\sigma \cdot L_1} & 0 & -\frac{1-\sigma}{\sigma \cdot L_h} & 0 \\ 0 & \frac{1}{\sigma \cdot L_1} & 0 & -\frac{1-\sigma}{\sigma \cdot L_h} \end{bmatrix} \cdot \begin{bmatrix} \Psi_{1d}(k) \\ \Psi_{1q}(k) \\ \Psi'_{2d}(k) \\ \Psi'_{2q}(k) \end{bmatrix} \quad (21)$$

The structure of the flux reconstructor is represented in Figure 7.

By means of the flux reconstructor, and the system of equations (10 - 13) the induced currents components are determined.

The power transferred to the liquid metal may be determined from the balance of power as follows:

$$P_{2tot} = [i]^T \cdot [u] - [i]^T \cdot [R] \cdot [i], \text{ în care: } [i] = \begin{bmatrix} i_{d1} \\ i_{q1} \\ i'_{d2} \\ i'_{q2} \end{bmatrix}, [u] = \begin{bmatrix} u_{d1} \\ u_{q1} \\ u'_{d2} \\ u'_{q2} \end{bmatrix}, [R] = \begin{bmatrix} R_1 & 0 & 0 & 0 \\ 0 & R_1 & 0 & 0 \\ 0 & 0 & R'_2 & 0 \\ 0 & 0 & 0 & R'_2 \end{bmatrix} \quad (22)$$

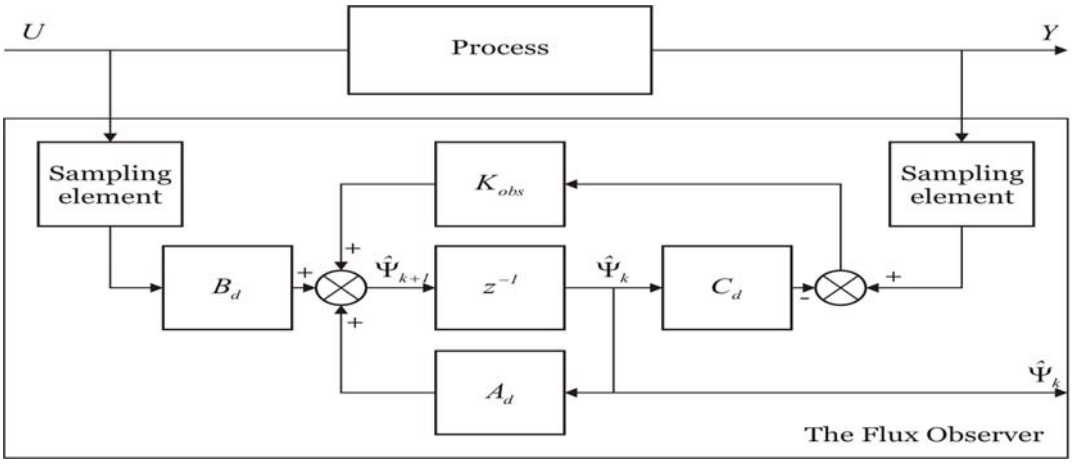

Figure 7. The flux observer.

The previous considerations have been implemented for a given induction electromagnetic pump designed with the procedure presented in [1]. The technical features of the pump are presented in Table 2.

Table 2. The technical features of the experimental induction electromagnetic pump.

No.	Denomination	Symbole	Units	Value
1	The rated supply voltage	U_{1N}	V	220
2	The rated frequency	f_{1N}	Hz	50
3	The rated flow rate	Q_{mN}	kg/s	22
4	No. of units	-	-	2
5.	Total power of a unit	P_t	W	9500
6.	The induced	-	-	cast-iron
7.	The pump's slope	s	o	10

The estimated values of the electric parameters of the pump are presented in Table 3. The computations have been performed according to the study [1]. To the practical implementation of the flux observer a software application has been conceived into the MatLab environment. The results are presented in Figures 8 and 9.

The currents components at start-up and in steady-state operation are presented in Figure 8.

Table 3. The estimated values of the electrical parameters of the experimental pump

No.	Denomination	Symbol	Units	Value
1	The phase resistance of the inductor	R_1	Ω	0.042361
2	The total inductance of the stator winding	L_1	H	0.0038067
3	The equivalent resistance of the melted metal referred to the number of stator turns	$R_2^{'}$	Ω	5.9419e-006
4	The linkage inductance	L_m	H	0.0028573
5.	The inductancies coefficient	σ	-	0.75061

As seen from the computations, the induced reaction is rather weak in comparison with the classical induction machine. In Figure 9 the estimate of the induced transferred power is presented. At start-up, i.e. when the melted metal doesn't moves, the transferred power has a maximum while at normal operation the power decreases three times.

4. CONCLUSIONS

Within this paper an analisys of state observers implementation to estimate the transferred power to the melted metal into an electromagnetic pump is presented. This estimation is possible if a model of the system is available. The proposed method allows the magnetic flux components reconstruction. The computations performed into the MatLab environment are compatible to the experiments and design data of the pump under study. The further researches could enhance pe usage of the observer to the melted metal flow rate estimation.

REFERENCES

[1] Peşteanu, O. *Jgheab electromagnetic pentru transportul fontei topite*. Universitatea Transilvania din Braşov. Contract de cercetare nr. 126/1984
[2] Fireţeanu, V. *Pomparea şi antrenarea electromagnetică a metalelor topite*. Editura Tehnică, Bucureşti, 1986
[3] Grellet, G., Clerc G. Actionneurs electriques, Edition Eyrolles, Paris, 2000.
[4] Henneberger, G. Electrial Machines 2. Aachen University 2002.
[5] Danila, A., A Direct- And Quadrature-Axis Approach To The Torque Estimation in an Eddy Currents Brake, In: International Symposium On Systems Theory, SINTES 13, Craiova – Romania, October 18-20 2007, pp 83 – 88.